SOME OBSERVATIONS OF SHELL-TYPE GALACTIC RADIO SOURCES

By E. R. Hill*

[*Manuscript received February* 9, 1967]

Summary

Radio evidence for two new supernova remnants in the Southern Milky Way is presented. Some new observations of the known supernova remnant, source 1439−62, and of the Rosette nebula, a shell source but not a supernova remnant, are also presented. The problem of finding model shells to fit the radio observations is considered and it is shown that the radio emission from 1439−62 is unlikely to originate in a shell with spherical symmetry.

I. Introduction

As a result of various sky surveys made with the Parkes radio telescope over the past three years, information has been accumulating which supports the recognition of three supernova remnant radio sources. Each of these sources is present in the 85·5 Mc/s MSH catalogue (Mills, Slee, and Hill 1958, 1960, 1961), where they are designated 09−3*2*, 14−6*3*, and 15−5*6*. Preliminary evidence concerning the supernova character of 14−6*3* was given by Hill (1964). In addition, observations of another shell-type source, the Rosette nebula (MSH 06+0*8*, NGC 2237), have been made. It is the intention here to present these observations, to derive where possible the angular dimensions of the emitting regions involved, and to outline the evidence supporting the supernova character of three of the sources.

II. Radio Observational Data

Surveys of all four objects noted above have been made at frequencies of 1410 and 2650 Mc/s with the Parkes 210 ft radio telescope, using the receivers developed by Gardner and Milne (1963) and Cooper, Cousins, and Gruner (1964). Scans were made over these objects using drive rates of $\frac{1}{4}$ or $\frac{1}{2}$ degree per minute and a receiver time constant of 1 sec. Contour maps of the sources derived from the 2650 Mc/s observations, where the aerial beamwidth is 7·5 min of arc, are presented in Figures 1(*a*) and 1(*b*) (Plate 1), and 1(*c*) and 1(*d*) (Plate 2). Owing to the weakness of the source in Figure 1(*a*), namely MSH 09−3*2*, or 0902−38 in the current nomenclature (see later), averages of about 10 repetitions of each scan were required to obtain the desired precision of mapping.

The contour maps of 1439−62 (Fig. 1(*b*), Plate 1) and 0629+04 (Fig. 1(*d*), Plate 2) have been superimposed on photographs of the corresponding regions of sky. In the case of 1439−62, the photograph is that obtained by B. Westerlund of the Mount Stromlo Observatory and shows clearly the three filamentary nebulosities that are associated with the radio source. The photograph upon which the contours of 0629+04 are superimposed is the blue print of the region taken from the Palomar Sky Atlas.

* Division of Radiophysics, CSIRO, University Grounds, Chippendale, N.S.W.

Aust. J. Phys., 1967, **20**, 297–307

Numerical data describing each object are listed in Table 1. Some explanatory comments on the table are necessary. In the first instance, the source name in column 1 is based on the celestial coordinates given in the next column, in accordance with the system introduced by Bolton, Gardner, and Mackey (1964). The coordinates given in column 2 refer to the centre of the source as a whole as judged by the outlying contours that surround the entire object. Where there are clearly defined peaks within the outlying contours, their coordinates have been listed separately in footnotes to the table. Galactic coordinates given in the subsequent column are in the new system. Secondly, the spectral indices have been deduced by combining the MSH data at 85·5 Mc/s with the present results at 1410 and 2650 Mc/s. Here the large frequency interval provided by the older observation has added materially to the precision of these indices. Thirdly, polarization data have been taken from Gardner and Davies (1966), and in each case these refer to the strongest component of the source rather than to the source as a whole. Finally, the apparent diameters refer to the rim of the source as deduced directly from the observations, and the circles used are shown on the contour maps. The estimated true angular diameters and shell thicknesses relate to the models fitted to the observations. There was insufficient angular resolution to make such a detailed interpretation of the source 1548−55 as was made of the other sources. These matters are discussed more fully in the next section.

III. Models of the Emitting Regions of the Sources

(a) *Assumptions and Computing Procedure*

With the exception of 1548−55, the sources are of sufficient angular size and display sufficient regularity of structure to allow rudimentary models of their emitting regions to be determined. The appearance of the contour maps of these sources suggests spherical symmetry, so that an attempt has been made to determine the radial distribution of volume emissivity that will best fit the observations in these cases. In addition, we will be assuming little internal absorption of radiation within the sources. This is clearly valid for the thermal source 0629+04, since the small value of the brightness temperature compared with the electron temperature ($\sim 10^4$ °K) implies a small optical thickness. Significant free-free absorption in the other sources is unlikely for the same reason.

Fig. 1.—Contour maps of the four sources obtained at a frequency of 2650 Mc/s with a beamwidth of 7·5 min of arc. The source identities and the factors to apply to convert contour labels to antenna temperatures are:

(*a*) 0902−38, 0·02 degK; (*b*) 1439−62, 0·14 degK;

(*c*) 1548−55, 0·50 degK; (*d*) 0629+04, 0·25 degK.

Contours of (*b*) 1439−62 are superimposed on a photograph of the region kindly supplied by Dr. B. Westerlund. The arrows point to faint nebulous filaments referred to in the text. Contours of (*d*) 0629+04 are superimposed on a blue print of the region from the Palomar Sky Atlas. All coordinates relate to epoch 1950·0.

SHELL-TYPE GALACTIC RADIO SOURCES

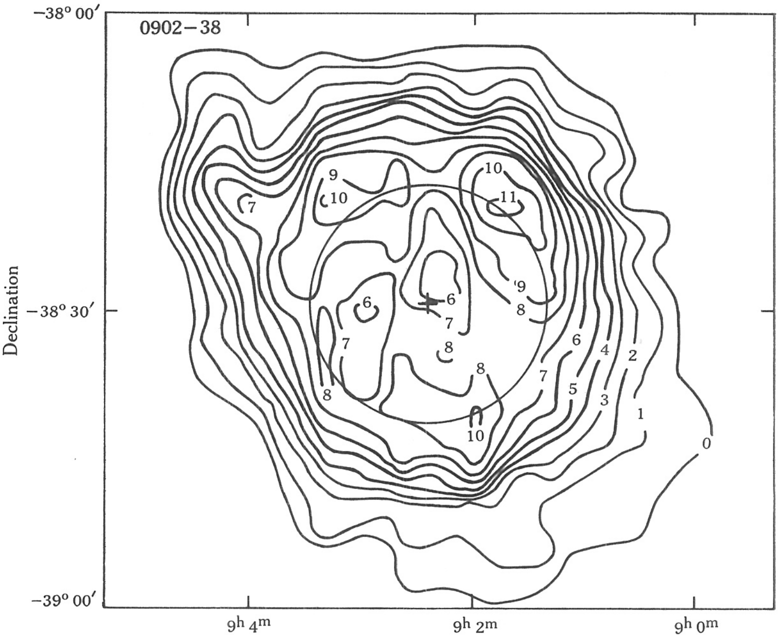

Fig. 1(*a*)

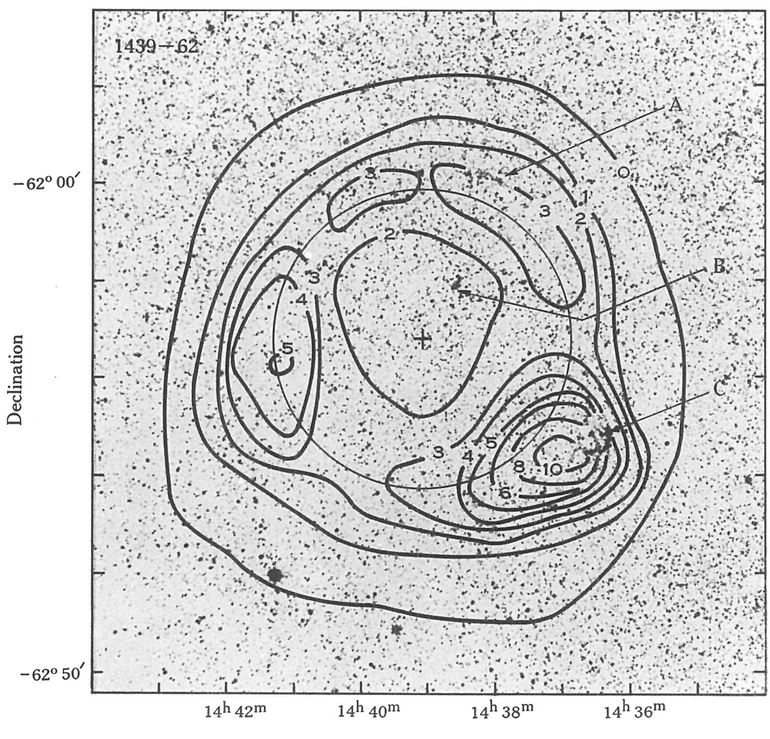

Fig. 1(*b*)

SHELL-TYPE GALACTIC RADIO SOURCES

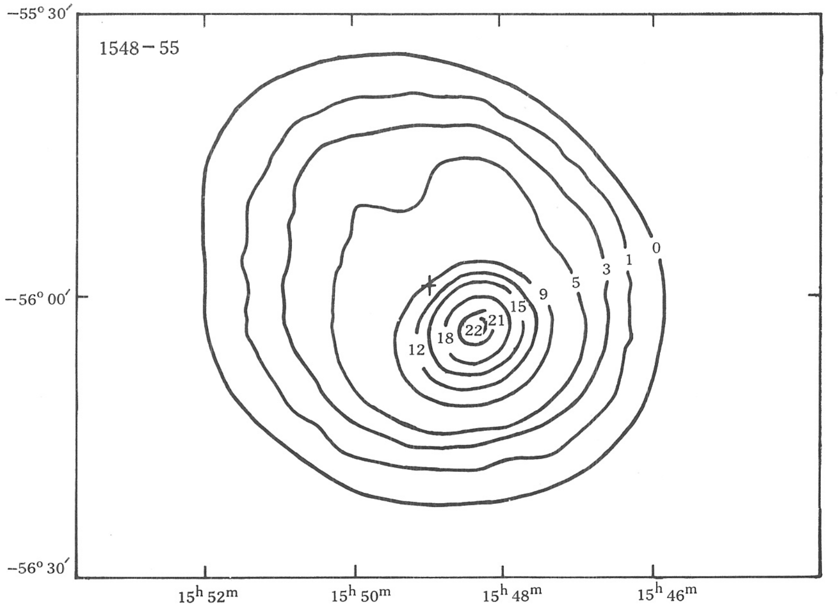

Fig. 1(*c*)

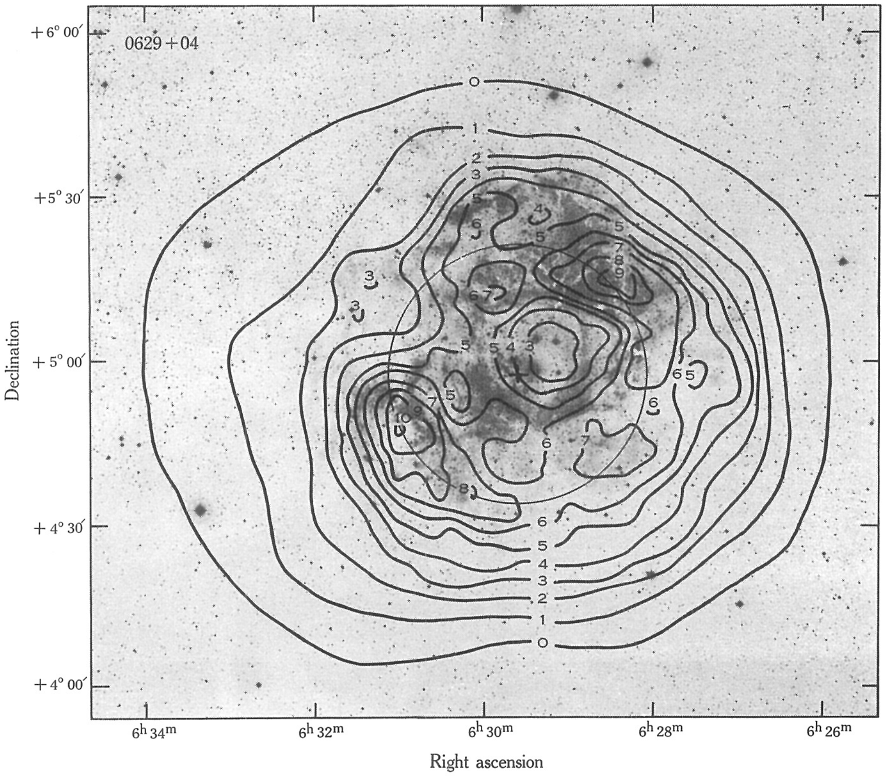

Fig. 1(*d*)

From our analysis it was hoped to get estimates of real angular sizes and, if shell structure were sufficiently evident, an estimate of the shell thickness. It is quite clear, however, that such a simple model is merely an approximation to reality and refers to the gross overall character of these objects. Around the rims of 0629+04, 0902−38, and 1439−62 there are obvious irregularities in emission, some of which lie outside the circle best fitting the rims. Another sign of these irregularities is the fact that the central temperatures are not always minima, for example, in 0902−38 and 0629+04. This indicates the presence of irregularities on the front and back surfaces of these sources. In addition, 0629+04 exhibits a deep rift in its perimeter.

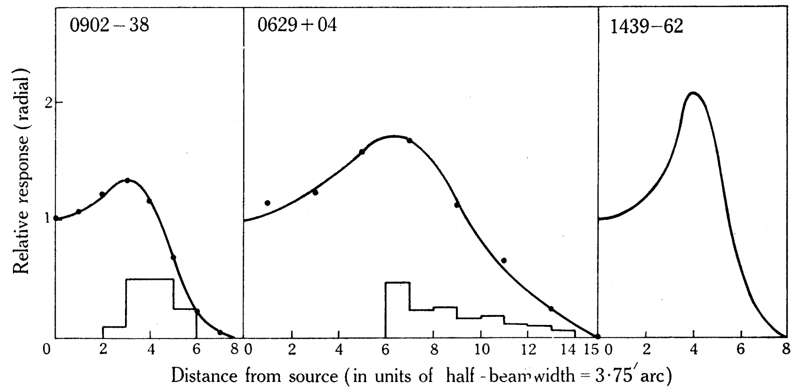

Fig. 2.—Radial distributions of observed brightness distributions of three of the sources derived from their contour maps. Superimposed on two of these is the computed volume emissivity distribution in histogram form. Note that for the sources 0902−38 and 0629+04 the model used was spherical. The dots outline the radial brightness distribution as computed back from the models.

To provide a criterion for determining the accuracy of the models, the radial distribution of the observed radio emission has been used; it was determined by averaging the aerial temperatures around circles of various radii centred on the positions given in Table 1. These distributions are shown as the continuous curves of Figure 2. It should be noted that in deriving them several features of the contour maps thought unusually unrepresentative of the sources have been omitted. These features are: (1) the narrow flare to the north-east of 0902−38; (2) the broad extension of 0629+04 to the east; and (3) the brightest region in the south-west portion of 1439−62.* All these features seem not to bear any connection with the gross symmetry characteristics with which we are primarily concerned. Indeed, the Rosette extension appears to be connected with faint diffuse optical emission stretching to at least several degrees to the east of the rather compact optical object. The feature

* Briefly, the effects of these features were eliminated in the derivation of the radial distributions of radio emission in the following ways. The effects of the flare on 0902−38 were subtracted out by interpolating the course of the contours adjacent to it before averaging temperatures around the circles. For 0629+04 no measurements were taken along circles passing between the 0 and 1 contours on the eastern side of the source, while for 1439−62 no temperatures were measured in the sector occupied by the bright region.

TABLE 1

CHARACTERISTICS OF FOUR SHELL-TYPE OR RING-TYPE GALACTIC RADIO SOURCES

(1)	(2)		(3)		(4)			(5)		(6)	(7)	(8)	(9)
	Coordinates (1950·0)				Flux Density (flux units)			Ang. Diam.					
	Celestial*		Galactic		85·5	1410	2650	Appar-ent	Est. True				
Source	R.A. h m s	Dec. ° ′	l °	b °	(Mc/s)			′	′	Spectral Index	Polarization (%)	Ring Thick-ness ′	Optical Identification
0902−38 (09−32)	09 02 22	−38 29	261·9	+5·5	25	8	7	25	44	−0·4	None	15	None
1439−62 (14−63)	14 39 08	−62 15	315·4	−2·3	110	30	20	31	52†	−0·5	2·9±0·5 (1410 Mc/s)	—	Supernova of A.D. 185? Faint filamentary nebulosity (see text)
1548−55 (15−56)	15 48 58	−55 59	326·3	−1·7	323	129	115	34×39	45	−0·3	0·8±0·5 (2650 Mc/s) 0·3±0·3 (1410 Mc/s)	—	None
0629+04 (06+08)	06 29 36	+04 57	206·4	−2·0	250	201	219	46	105	0·0	—	30	NGC 2237 Rosette nebula

* Note for 0902−38: The principal peak is centred at $09^h 01^m 37^s$, −38°19′, whilst lesser peaks occur at $09^h 03^m 16^s$, −38°19′, and $09^h 01^m 52^s$, −38°41′.

1439−62: The principal peak is centred at $14^h 37^m 02^s$, −62°28′.

1548−55: The principal peak is centred at $15^h 48^m 30^s$, −56°04′.

0629+04: The principal peak is centred at $06^h 31^m 01^s$, +4°47′, whilst there are less prominent peaks at $06^h 28^m 28^s$, +4°43′, $06^h 28^m 24^s$, +5°14′, and $06^h 29^m 55^s$, +5°12′, around the periphery of the source.

† This estimate refers to a disk model and not to a spherically symmetrical model as in the other cases.

in 1439—62 is evidently connected with the small nebulosity displaying much higher curvature than the main part of the nebula. The effects of the remaining irregularities in the contour maps may be expected to be removed to a great degree in the averaging process used to derive the curves of Figure 2.

The procedure in determining the emissivity distribution has been to imagine each source divided up into concentric shells of thickness equal to half a beamwidth. Then the responses of a Gaussian aerial pattern to each of these shells is computed. It is then only necessary to combine the responses of these shells, each with an associated weight, in such a way that the sum of the responses matches the observed radial distribution to a tolerable precision. The resulting weights give the distribution of volume emissivity in the model source.

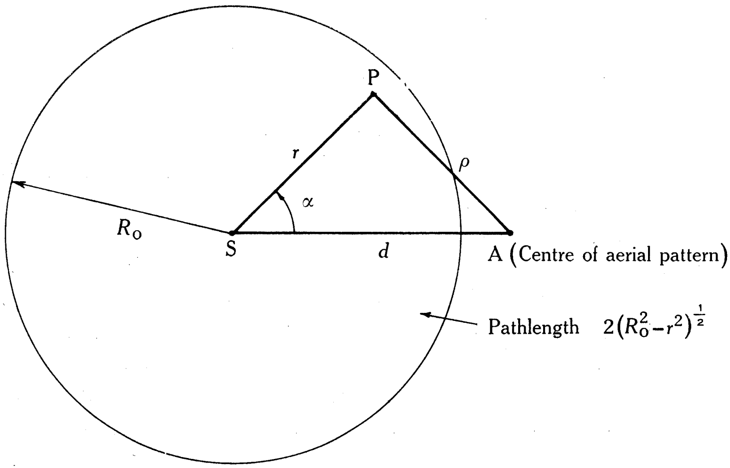

Fig. 3.—Illustrating the notation used in the calculation of the response of the aerial to a spherical radio source with uniform volume emissivity.

The response of an aerial to a spherical shell of radiating matter is merely the difference of the responses of the aerial to two spheres of radii equal to the inner and outer radii of the shell and volume emissivities equal to that of the shell. In Figure 3 is illustrated such a sphere of radius R_0, and we have supposed the surface brightness to be proportional to the pathlength through the sphere, that is, that there is no re-absorption of radiation within the source. The aerial pattern $\exp(-k\rho^2)$, is supposed centred on the direction A distant d from the centre of the sphere. The response to this sphere as a function of d is simply

$$2\int_0^{R_0}\int_{-\pi}^{+\pi} r(R_0^2-r^2)^{\frac{1}{2}}\exp\{-k(r^2+d^2-2rd\cos\alpha)\}\,\mathrm{d}r\,\mathrm{d}\alpha\,,$$

where the variables r and α are as identified in Figure 3. The α-integration yields a Bessel function, so that the response becomes

$$4\pi\int_0^{R_0} r(R_0^2-r^2)^{\frac{1}{2}}I_0(2krd)\exp\{-k(r^2+d^2)\}\,\mathrm{d}r\,.$$

This result can be put in a more flexible form by expressing all angular distances in units of half the half-power beamwidth of the aerial. When this is done the response is, apart from a constant factor,

$$R(R_0';d) = \int_0^{R_0'} r'(R_0'^2-r'^2)^{\frac{1}{2}} I_0(2Mr'd')\exp\{-M(r'^2+d'^2)\}\,\mathrm{d}r'\,,$$

where $M = \log_e 2$ and the primes indicate that the new units are being used. The response R_s of the aerial to a shell of inner and outer radii R_i' and R_o' is then

$$R_s(R_i', R_o'; d') = R(R_o'; d') - R(R_i'; d')\,.$$

For convenience, for future analyses of a similar nature to the present one, a table of the function

$$R(R'+1\cdot 0;\, d') - R(R';\, d')$$

is provided in the Appendix (Table A1).

(b) *Results of Model Calculations*

The radial distributions of volume emissivity derived in the above manner for the sources 0902−38 and 0629+04 are depicted in histogram form in Figure 2. It should be remembered that the unit along the abscissa is one-half the half-power beamwidth of the aerial, 3·75 min of arc in the present case. Source responses computed from the models are outlined by the dots in this figure. On account of inaccuracies in the observed data, no attempt was made to achieve an exact fit between the model and the observed responses. For this reason our derived emissivities have an uncertainty of about 5–10%, since variations of this amount in the emissivities will still yield a tolerable fit to the radial brightness distributions adopted. Both sources clearly represent thick shell-like emitting regions, and from them the true shell thicknesses and diameters in Table 1 were estimated. It might be added that the volume emissivity for 0629+04 shows a definite tendency to increase towards the inner surface of the shell.

In the case of the source 1439−62, however, it was found that the type of model so far discussed, the spherically symmetrical model, could not possibly fit the observed radial distribution of emission. The simplest way to illustrate the impossibility is to search Table A1 in the Appendix for a shell producing a maximum response near $d' = 4$, as does 1439−62. According to the table the required shell would have an inner radius between 4·0 and 5·0. However, such a shell would not yield the rim/centre temperature ratio of 2·1 exhibited by the source; the model shell rim/centre ratio would at most be about 1·7 according to the table. Further calculation shows that if thinner shells than those considered in the table are used, the highest ratio would only be slightly higher. In fact, only in the direction of the gap on the western side of 1439−62 could the observed radial brightness distribution be matched by our model.

Failure of the spherically symmetrical model in the case of source 1439−62 raises the question of what sort of models might be used to describe the source. If a shell-type model is to be retained, as is suggested by physical arguments, then the observed radio emission could be explained by an enhancement of the volume emissivity in the shell towards the plane through the physical centre of the source and perpendicular to the line of sight. To describe such a model would require additional parameters, which could not be assessed uniquely from our observations. An extreme case of such an interpretation is that in which the source is regarded as a disk lying perpendicular to the line of sight. In these circumstances the best approximation to the distribution of volume emissivity across the disk is the observed brightness distribution adopted for this source in Figure 2.

In so far as the source 1548−55 is concerned, an analysis like the above is seriously hampered by the uncertainty of the brightness distribution of the source near its centre. Here with the present beamwidth an off-centre bright region is influencing the central temperature. Further observations with higher angular resolution should improve the situation. We have, however, made a rough estimate of the emissivity distribution using the observed brightness distribution along a radius from the centre pointed in the north-easterly direction, modified so that it is flat within a few minutes of arc from the source centre. This yielded a constant volume emissivity out to about 22·5 min of arc, which value was adopted as the angular radius of the source.

IV. Discussion

The nature of the source 0629+04 (the Rosette nebula) has already been discussed in some detail by Menon (1962) and by Bottinelli and Gougenheim (1964). It is an HII region radiating thermally at radio frequencies, and this interpretation is supported by the spectral index in Table 1. The observations described here have provided a picture of the distribution of radio radiation associated with the nebula of somewhat higher angular resolution than those previously available. Ensuing from this is an improved model of the distribution of emissivity within the source. This model shows that the emissivity is concentrated towards the inner surface of the shell within which emission from the source is concentrated.

The sources 0902−38, 1439−62, and 1548−55 are characterized by a definitely non-thermal radio spectrum, and at present this appears to be the strongest indication that they are galactic supernova remnants radiating at radiofrequencies by the synchrotron process. In the case of 1439−62 we have optical confirmation of this from the work of Westerlund (1966) (see also the discussion following Hill 1964), who photographed filaments typical of supernova remnants around the source (see Fig. 1(*b*), Plate 1). Further confirmation is available from the radio polarization measured for the strongest part of this source. Finally, the contour maps of the sources 0902−38 and 1439−62 have appearances very similar to such well-established supernova remnants as Cassiopeia A and the Cygnus Loop. From present observations source 1548−55 may well display these features under examination with higher angular resolution.

No optical identifications of 0902−38 and 1548−55 have so far been possible. Furthermore, since both appear to be supernova remnants, the catalogues of Ho

Ping-Yü (1962) and Hsi Tse-Tsung and Po Shu-jen (1965), which list descriptions of ancient astronomical events derived from Chinese, Japanese, and Korean sources, have been examined, but they have failed to reveal any event likely to be related to either radio source. In regard to 1439−62, however, the entries 109 and 15 in the respective catalogues refer to an event, almost without doubt a supernova explosion, that occurred in 185 A.D. close to the position of this source. This fact was first noticed by Westerlund (1966), using an earlier catalogue of ancient astronomical events

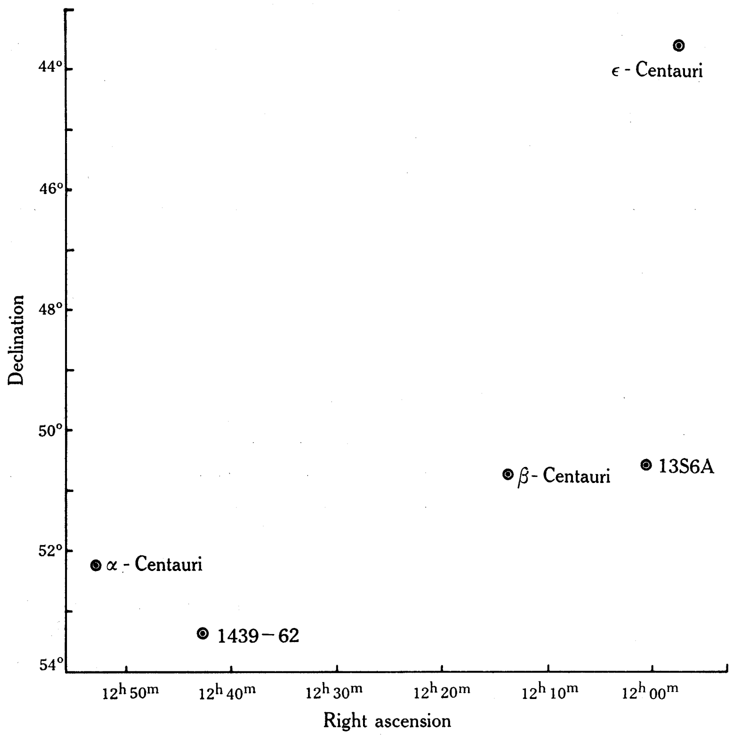

Fig. 4.—The relative positions of the sources 1439−62 and 13S6A and the stars α-, β-, and ε-Centauri as estimated for epoch 185 A.D.

by Hsi Tse-Tsung (1958), and he identifies the event with the radio source. Previously, Shklovsky (1954) had connected another radio source, 13S6A, with the same event. The source 13S6A is a strong non-thermal radio source (presumably galactic, on account of its low galactic latitude) that exhibits radio polarization (2·3% at 11 cm, Gardner and Davies 1966). It is an elongated source with its maximum dimension less than 15 min of arc, and so far it has not been identified optically. Both radio sources are close to the region of sky Nan-Mên (apparently closely associated with the stars α-, β-, and ε-Centauri) where the event took place. This is shown in Figure 4, where we have plotted the relative positions of the three stars and the two radio sources for the epoch 185 A.D. In deriving Figure 4 no allowance could be made for the proper motions of the radio sources, but it should not be very inaccurate on this account, except in the unlikely case that the sources have excessively large proper motions.

Thus it appears that there are two likely contending radio sources for association with the event of 185 A.D. At present 1439−62 seems favoured, principally because it is associated with optical filamentary nebulosities of the supernova type.

Finally, we make a few remarks concerning the significance of our attempts to make models of the emitting regions of the non-thermal radio sources 0902−38, 1439−62, and 1548−55. It should first of all be stressed that the models refer only to the sources of radiation that are observed by us. Because of the manner in which the synchrotron mechanism beams the emitted radiation, some regions in which the process is active may be invisible to an observer, e.g. regions in which the magnetic field is along the line of sight. Not enough is known at the present time of conditions within supernova remnants to be able to assess the extent to which the radiation-beaming characteristic of the synchrotron process mars our radio models of these sources. Our models of supernova remnant radio emission must therefore be regarded as provisional. If future studies show for at least some of these sources that conditions are such that radiation beaming is not an important factor in the derivation of the models, then these efforts in constructing them will be completely justified.

V. Acknowledgments

The author wishes to express his thanks to Dr. B. Westerlund for his cooperation in photographing fields in which the sources lie; to Mr. M. Beard, who cooperated in obtaining the observations; and to Miss J. Spells, who organized much of the digital computer work done in connection with the contour maps and tables presented here.

VI. References

Bolton, J. G., Gardner, F. F., and Mackey, M. B. (1964).—*Aust. J. Phys.* **17**, 340.

Bottinelli, L., and Gougenheim, L. (1964).—*Annls Astrophys.* **27**, 685.

Cooper, B. F. C., Cousins, T. E., and Gruner, L. (1964).—*Proc. Instn Radio Engrs Aust.* **25**, 221.

Gardner, F. F., and Davies, R. D. (1966).—*Aust. J. Phys.* **19**, 441.

Gardner, F. F., and Milne, D. K. (1963).—*Proc. Instn Radio Engrs Aust.* **24**, 127.

Hill, E. R. (1964).—Symp. IAU–URSI No. 20, p. 107.

Ho Ping-Yü (1962).—*Vistas Astr.* **5**, 127.

Hsi Tse-Tsung (1958).—*Smithson. Contr. Astrophys.* **2**, 109.

Hsi Tse-Tsung and Po Shu-jen (1965).—*Acta astr. sin.* **13**, 1. (See English translation by N.A.S.A., NASA TT F-388.)

Menon, T. K. (1962).—*Astrophys. J.* **135**, 394.

Mills, B. Y., Slee, O. B., and Hill, E. R. (1958).—*Aust. J. Phys.* **11**, 360.

Mills, B. Y., Slee, O. B., and Hill, E. R. (1960).—*Aust. J. Phys.* **13**, 676.

Mills, B. Y., Slee, O. B., and Hill, E. R. (1961).—*Aust. J. Phys.* **14**, 497.

Shklovsky, I. S. (1954).—*Dokl. Akad. Nauk SSSR* **94**, 417.

Westerlund, B. E. (1966).—Symp. on Radio and Optical Studies of the Galaxy. (Eds J. V. Hindman and B. E. Westerlund.) p. 78.

TABLE A1

THE FUNCTION $\int_{R'}^{R'+1\cdot 0} r'(R'^2-r'^2)^{\frac{1}{2}} I_0(2Mr'd') \exp\{-M(r'^2+d'^2)\}\,dr'$

R'	d': 0·0	1·0	2·0	3·0	4·0	5·0	6·0	7·0	8·0	9·0	10·0	11·0	12·0	13·0	14·0	15·0
0·0	2·57(−1)	1·52(−1)	3·02(−2)	1·88(−3)												
1·0	8·55(−1)	7·25(−1)	3·41(−1)	6·34(−2)	3·84(−3)											
2·0	8·58(−1)	9·34(−1)	9·03(−1)	4·59(−1)	8·81(−2)	5·41(−3)										
3·0	7·78(−1)	8·36(−1)	1·02	1·05	5·55(−1)	1·08(−1)	6·75(−3)									
4·0	7·51(−1)	7·76(−1)	8·80(−1)	1·11	1·18	6·37(−1)	1·26(−1)	7·92(−3)								
5·0	7·41(−1)	7·55(−1)	8·06(−1)	9·35(−1)	1·20	1·30	7·10(−1)	1·42(−1)	8·98(−3)							
6·0	7·34(−1)	7·44(−1)	7·77(−1)	8·44(−1)	9·91(−1)	1·29	1·41	7·76(−1)	1·56(−1)	9·94(−3)						
7·0	7·31(−1)	7·39(−1)	7·61(−1)	8·04(−1)	8·83(−1)	1·04	1·37	1·51	8·37(−1)	1·70(−1)	1·08(−2)					
8·0	7·29(−1)	7·34(−1)	7·51(−1)	7·83(−1)	8·35(−1)	9·23(−1)	1·10	1·45	1·61	8·94(−1)	1·82(−1)	1·17(−2)				
9·0	7·27(−1)	7·31(−1)	7·45(−1)	7·68(−1)	8·06(−1)	8·66(−1)	9·62(−1)	1·15	1·52	1·70	9·48(−1)	1·94(−1)	1·24(−2)			
10·0	7·26(−1)	7·30(−1)	7·40(−1)	7·59(−1)	7·88(−1)	8·31(−1)	8·96(−1)	1·00	1·20	1·59	1·78	1·00	2·05(−1)	1·32(−2)		
11·0	7·26(−1)	7·28(−1)	7·37(−1)	7·53(−1)	7·76(−1)	8·09(−1)	8·56(−1)	9·26(−1)	1·04	1·25	1·66	1·86	1·05	2·15(−1)	1·39(−2)	
12·0	7·24(−1)	7·27(−1)	7·35(−1)	7·47(−1)	7·66(−1)	7·93(−1)	8·30(−1)	8·82(−1)	9·56(−1)	1·07	1·29	1·73	1·94	1·09	2·25(−1)	1·46(−2)
13·0	7·25(−1)	7·26(−1)	7·32(−1)	7·43(−1)	7·59(−1)	7·81(−1)	8·11(−1)	8·51(−1)	9·07(−1)	9·86(−1)	1·11	1·34	1·79	2·01	1·13	2·34(−1)

Appendix

The integral involved in calculating the response of a Gaussian aerial pattern to a spherical source having uniform volume emissivity (Section III) appears to be of sufficient interest to warrant tabulation. Table A1 is therefore provided and gives the value of

$$\int_{R'}^{R'+1\cdot 0} r'(R'^2-r'^2)^{\frac{1}{2}} I_0(2Mr'd') \exp\{-M(r'^2+d'^2)\}\,\mathrm{d}r',$$

where $M = \log_e 2$. The precision and particularly the extent of the entries have been decided on the basis of the current application. Note that an entry such as $2\cdot 57(-1)$ means $2\cdot 57\times 10^{-1}$.